JOURNAL OF PROPULSION AND POWER
Vol. 15, No. 1, January–February 1999

Ignition Delay Times of Ram Accelerator CH_4/O_2/Diluent Mixtures

Eric L. Petersen,* David F. Davidson,† and Ronald K. Hanson‡
Stanford University, Stanford, California 94305

An experimental study was performed to determine ignition delay times for CH_4/O_2/diluent mixtures and conditions relevant to forebody combustion on ram accelerator projectiles. All measurements were performed in the reflected-shock region of a high-pressure shock tube. Temperatures from 1040 to 1600 K and pressures between 35 and 260 atm were studied, and the CH_4/O_2/diluent mixtures had an equivalence ratio of 0.4, 3.0, or 6.0 with either N_2, Ar, or He as the bath gas. Reaction progress was monitored primarily via piezoelectric pressure transducer and visible emission. For each mixture and condition, the ignition developed as a strong ignition front beginning at the endwall with little or no preignition deflagration. Ignition delay time (τ_{ign}) correlations were generated for each mixture and the entire data set; the latter correlation indicates that ignition delay is dependent only on the fuel and oxidizer concentrations and, therefore, not on the diluent species or concentration. At temperatures below approximately 1300 K for the fuel-rich mixtures, the Arrhenius temperature dependence of τ_{ign} changes from an average activation energy of 32.7 kcal/mol, at higher temperatures, to approximately 19.0 kcal/mol, at lower temperatures. The transition occurs at higher temperatures as the pressure is increased, and is indicative of a shift in chain-branching kinetics between the high- and intermediate-temperature regimes.

Introduction

SINCE its inception nearly 10 years ago,[1] the ram accelerator concept has been the subject of active research. The overall performance and stability of the device,[2,3] the aerodynamic design of the projectile,[4–6] and the gasdynamic properties of the propellant mixture[6,7] have received particular attention. The ultimate goal is to successfully accelerate projectiles to ultrahigh velocities (1–12 km/s).[1] The ram accelerator projectile is injected by various means, at supersonic speeds, into the high-pressure (10–100 atm) combustible mixture. Shock waves formed between the projectile body and the tube walls lead to ram compression, shock-induced combustion, and thrust. A review of the possible gasdynamic operating regimes of the ram accelerator can be found in Hertzberg et al.[1,8]

The gaseous propellant is typically a rich (ϕ = 2.0–6.0) mixture of hydrocarbon fuel or hydrogen, molecular oxygen, and a bath gas such as nitrogen, helium, or carbon dioxide. Of the possible fuels, CH_4 is used most often and will be emphasized in the present study. For example, the University of Washington[6,7] has utilized mixtures such as $2.8CH_4 + 2O_2 + 5.8N_2$ and $4.5CH_4 + 2O_2 + 3.9He$, and the standard Army Research Laboratory (ARL) mixture[9] is currently $3CH_4 + 2O_2 + 10N_2$. These propellant combinations contain a relatively low diluent concentration and are tailored to provide a desired Chapman–Jouguet (CJ) detonation velocity, sound speed, and heat release. Recent studies have also been performed with a fuel-lean (ϕ = 0.4) $0.4CH_4 + 2O_2 + 8N_2$ mixture.[10,11]

In the ideal scenario, all heat release occurs downstream of the oblique shock/detonation located near the projectile midsection. Equilibrium chemistry is generally assumed when evaluating and predicting one-dimensional ram accelerator performance, so most studies to date have placed less importance on the chemical kinetics of the propellant combination. However, Nusca and Kruczynski[12] recently emphasized the role of ignition delay time on the generation of adequate thrust levels. It was noted that compression of the gas downstream of the bow shock can precipitate premature combustion on the projectile forebody, where temperatures as high as 1300 K are expected. Forebody combustion has been witnessed experimentally,[13] and leads to a negative thrust component and possible unstart.[12] The abrupt deceleration resulting from unstart is often experienced during tests in the superdetonative regime, sometimes leading to catastrophic failure of the projectile.[14] An ideal ram accelerator mixture should therefore have a long enough ignition delay time to prevent forebody combustion. To properly design such a configuration, a priori knowledge of the mixture's ignition delay time characteristics is essential. Such information is of increasing importance to numerical modelers who are beginning to incorporate finite rate chemistry.[4,12,15–18]

Many experimental and analytical studies have been performed on the ignition and oxidation of methane, mostly at pressures near or below 1 atm and at temperatures above 1400 K. Ignition times covering a large range of conditions have been measured in low-pressure shock tubes, and the associated detailed kinetics models of low-pressure methane oxidation now include well over 100 reactions.[19,20] Spadaccini and Colket[21] give a thorough review of earlier CH_4 ignition investigations. In a recent study conducted in our laboratory,[22] methane oxidation data at higher pressures were obtained in the form of species profiles and ignition delay times. The data cover a wide range of pressure (10–480 atm), temperature (1400–2000 K), equivalence ratio (0.5–4.0), and argon dilution (≥90%), and the experimental results compare favorably with calculations using a modern chemical kinetics model.[23]

Nonetheless, ram accelerator ignition differs from previous ignition time studies in several ways: 1) the forebody region sees postshock pressures near 100 atm or more; 2) the mixtures are predominately fuel-rich (ϕ = 2.0–6.0), where the kinetics are less known[22,24]; 3) at the temperatures of interest to forebody combustion (<1400 K), ignition occurs in an intermedi-

Presented as Paper 96-2681 at the AIAA/ASME/SAE/ASEE 32nd Joint Propulsion Conference, Lake Buena Vista, FL, July 1–3, 1996; received Oct. 15, 1997; revision received April 8, 1998; accepted for publication Aug. 4, 1998. Copyright © 1998 by the American Institute of Aeronautics and Astronautics, Inc. All rights reserved.

*Graduate Research Assistant; currently Member of the Technical Staff, The Aerospace Corporation, El Segundo, CA 90245-4691. Member AIAA.

†Senior Research Associate, Department of Mechanical Engineering. Member AIAA.

‡Professor, Department of Mechanical Engineering. Fellow AIAA.

ate-temperature, high-pressure regime where no CH_4/O_2 ignition data exist[21]; and 4) the diluent gas is comprised of comparatively low levels (<70%) of N_2, He, CO_2, or even H_2, whereas most ignition and kinetics data have been measured in highly dilute argon baths. Hence, ram accelerator combustion occurs in a region where ignition data are scarce and the kinetics are poorly known.[24]

With the goal of providing the desired information on ram accelerator ignition chemistry, ignition-delay measurements were performed in our High Pressure Shock Tube Laboratory for a variety of propellant combinations. This paper presents the experimental results of the investigation. The details of the experimental apparatus and procedure are described, followed by the ignition delay time results and interpretation. Although the mixtures explored herein are based on those used at ARL, the results are applicable to similar ram accelerator mixtures employed elsewhere. The data and analyses presented herein supersede the earlier work of Petersen et al.[25,26]

Experiment

Apparatus

All ignition delay times were measured in the reflected-shock region of a 5-cm-diam, helium-driven shock tube. Prescored steel or aluminum diaphragms of various thickness (1–5 mm) were utilized, and the tube was operated in both the single- and double-diaphragm modes. Test pressures as high as 1000 atm are achievable in this facility. Four time-interval readings (using 5 PCB 113A pressure transducers and 4 Fluke PM6666 counters) were used to determine the velocity profile of the incident shock wave. Attenuation of the incident shock was typically 2–3%/m near the endwall. Further details of the shock tube are presented elsewhere.[27]

Various measurement techniques were employed throughout the investigation to monitor the reaction progress. Measurements included 1) pressure (PCB 113A), 2) infrared (IR) emission near 3.3 μm, 3) visible emission (Si photodiode), and 4) laser extinction (He–Ne at 632.8 nm). The 3.3-μm emission was from the initial methane present in the mixture (ν_3 fundamental vibration), higher hydrocarbons formed during reaction, and the spectrally broad emission from soot; the visible emission contribution came mostly from soot luminosity, CH (431 nm), and C_2 (517 nm); and the laser light extinction was caused by the formation of hydrocarbon particles (soot) and/or increased density i.e., refractive index, fluctuations from the reaction zone behind the reflected shock wave. The presence of CH was verified in selected experiments via interference filters. Of the preceding methods, the pressure transducer was always used, and visible emission was the optical technique most often applied.

Figure 1 displays sample pressure traces and illustrates the definition of ignition delay time. The ignition times derived from the optical diagnostics always agreed with the pressure-derived ones to within a few percent; further comparisons between the pressure and emission measurements are provided next. For most experiments, the measurement ports were located 20 mm from the endwall, although selected pressure measurements were also performed at the endwall.

The mixtures were based on recent ram accelerator tests performed at ARL.[28] In addition to N_2 and He as diluents, argon was also used in the present study to 1) explore the effect of bath gas on ignition delay time; 2) enable comparisons with the large amount of $CH_4/O_2/Ar$ data available; and 3) because argon is the preferred shock-tube driven gas (higher P_5 for a given driver pressure, longer test time, and fewer nonideal gasdynamic effects). Table 1 provides a list of the propellant mixtures. Each was prepared in aluminum cylinders using partial pressures. The purity of the Matheson N_2 and He were 99.99 and 99.995%, respectively, and the argon was an ultra high purity (UHP) grade (99.999%). The oxygen was 99.996%, and the UHP methane was 99.97% pure. While most

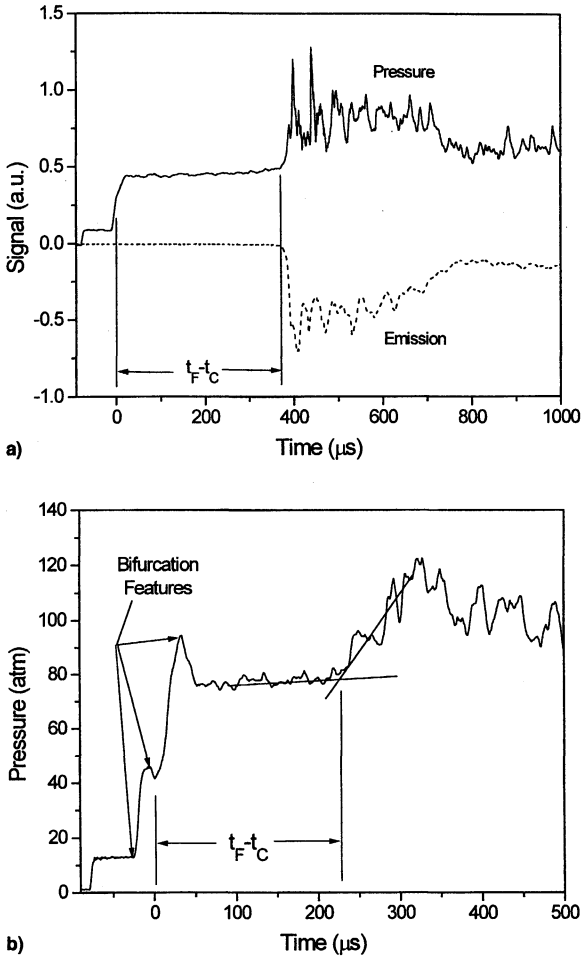

Fig. 1 Sample pressure and visible emission traces showing definition of ignition delay time and the reflected-shock bifurcation. t_C is the time of normal reflected-shock passage, and t_F is the time of arrival of the ignition front: a) $3CH_4 + 2O_2 + 10Ar$, 1179 K, 106 atm and b) $3CH_4 + 2O_2 + 10N_2$, 1334 K, 76 atm.

of the Table 1 mixtures are very fuel-rich ($\phi \geq 3$), one fuel-lean mixture was also studied (mixture 1, $\phi = 0.4$).

Procedure

Because impurities (particularly higher hydrocarbons) are known to drastically decrease the ignition delay time of CH_4/O_2 mixtures,[21,29] care was taken during the experiments to minimize their presence. The bottled methane contained fewer than 300 ppm total impurities, and so the Table 1 mixtures contained much less than 100 ppm of higher hydrocarbons or H_2O. However, the ram accelerator mixtures produced noticeable amounts of soot and liquid hydrocarbons at reflected-shock conditions, and early tests found this residue to accelerate the ignition delay time of the following run. Therefore, the inner surfaces of the shock tube were wiped cleaned with acetone after each experiment. As standard procedure, the driven section was turbomolecular pumped below 10^{-4} torr before each run.

Reflected Shock Properties

The conditions behind the reflected shock wave were determined from the incident-shock velocity (extrapolated to the endwall) using the one-dimensional shock relations and the Sandia thermodynamic database. Because of the high pressures encountered, the real-gas correction data of Schmitt and Butler[30] and the Peng–Robinson equation of state (EOS) were applied to the reflected-shock calculations per the method of Davidson and Hanson.[31] Recent experiments have shown that the Peng–Robinson EOS adequately models the real-gas prop-

Table 1 Mixtures investigated and ignition delay time correlations

		High-temperature correlation[a]			Low-temperature correlation[a]		
Number	Mixture	A	x	E, kcal/mol	A	x	E, kcal/mol
1	$0.4CH_4 + 2O_2 + 8Ar$	8.62×10^{-12}	−0.87	27.8	——	——	——
2	$3CH_4 + 2O_2 + 10N_2$	7.34×10^{-15}	−1.23	40.6	1.31×10^{-12}	−1.67	19.4
3	$3CH_4 + 2O_2 + 10Ar$	Same as above			Same as above		
4	$3CH_4 + 2O_2 + 6N_2$	1.20×10^{-13}	−1.29	30.6	4.11×10^{-13}	−1.74	19.7
5	$3CH_4 + 2O_2 + 6Ar$	Same as above			Same as above		
6	$6CH_4 + 2O_2 + 4He$	3.07×10^{-15}	−1.46	37.5	[b]		
7	$3CH_4 + 2O_2 + 4N_2 + 8He$	6.76×10^{-14}	−1.22	34.5	[b]		

[a]Correlation is of the form: $\tau_{ign} = A[M]^x \exp(E/RT)$, where $[M] = P/RT$ in mol/cm^3. [b]Few data were taken in low-temperature regime.

erties of argon at relevant shock-tube pressures and temperatures.[32] However, for the extreme conditions of this investigation (260 atm, 1300 K), the temperature and pressure predictions are only 3 K and 1.5 atm lower, respectively, than those obtained assuming an ideal gas. Thus, the reflected-shock temperatures (T_5) calculated in the present study are not expected to be sensitive to the specific real-gas EOS.

Using the procedure outlined in the preceding text, the overall error in the initial value of T_5 is approximately 5 K. However, shock attenuation causes T_5 and P_5 to increase slightly with time.[33] This nonideal effect was minimized by keeping most ignition delay times below 400 μs, where the estimated average T_5 error over the entire induction period was less than 15 K. Further details on reflected-shock temperatures in the Stanford High Pressure Shock Tube are provided by Petersen.[34]

Because the Table 1 ram accelerator mixtures contained large percentages of di- and polyatomic gases, nonideal gasdynamic effects were encountered. Their impact was felt through bifurcation of the reflected shock wave, which routinely occurs in shock tubes with polyatomic test gases.[35] The reflected shock wave forms a bifurcated foot when interacting with an incident-wave boundary layer whose total pressure is too low to allow passage through a normal shock wave. As seen in Fig. 1b, the bifurcation produces a double rise in the sidewall pressure, obscuring the arrival of the main reflected shock. The time of normal shock wave passage, t_c, was calculated from the sidewall pressure measurement using the procedure outlined in Refs. 34 and 36. In brief, time zero was defined as the time of arrival of the normal portion of the reflected shock wave. This time was obtained from a combination of 1) features in the measured pressure trace; 2) a correlation of measured bifurcation step height, obtained for a wide range of test-gas specific heat ratios and molecular weights; and 3) one-dimensional gasdynamic theory.

Strong Ignition

When a highly exothermic reaction occurs in the stagnation region behind a reflected shock wave, the ensuing adiabatic explosion generates a blast wave that propagates from the endwall. The resulting detonation-like structure, commonly referred to as strong ignition, was first examined by the authors of Refs. 37–41 in H_2/O_2-based mixtures. The definitions of strong and weak ignition were experimentally redefined using H_2/O_2-,[42–45] hydrocarbon- (n-heptane and iso-octane),[46] and CH_4/O_2-based[47–49] mixtures. Analytical studies were conducted by Cohen et al.,[50] Oran et al.,[51] and Oran and Boris.[52]

Weak, or mild, ignition is characterized by the appearance of distinct deflagration zones behind the reflected shock wave, accompanied by a very mild, if any, pressure rise.[42,46,48] These localized, inhomogeneous flame kernels are suspected to originate from nonuniformities and/or disturbances in the flow, such as turbulence or diaphragm fragments. Conversely, strong ignition corresponds to the near-sudden appearance of a shock or blast wave starting at the endwall.[39,42,49] This blast wave exhibits the characteristics of a detonation, wherein a shock wave is driven by a flame front. Flow visualization of the process shows that strong ignition tends to occur at the endwall nearly homogeneously across the entire shock-tube cross section, accompanied by an often sharp increase in pressure. The demarcation between weak and strong ignition depends primarily on the initial temperature and the exothermicity of the mixture.[46,49]

More recently, reflected-shock ignition tests were performed at pressures up to 49 atm for hydrocarbon mixtures of interest in internal combustion engine research.[53–58] This further refinement of strong ignition, particularly at high pressure, is of direct significance to the experiments herein. Using a combination of pressure, CH emission (431 nm), and schlieren photographs, several distinct phases of strong and mild ignition were identified and found to depend strongly on the temperature and the specific fuel under consideration. In general, mild ignition was observed to occur at the lowest temperatures and is evident by a very gradual, smooth increase in pressure and visible emission.[54,57] At higher temperatures, a transition to detonation was observed, indicating strong ignition.[53,54] Dramatic pressure spikes and oscillations, much like what is shown in Fig. 1a, normally accompany strong ignition.

However, the schlieren measurements of Pfahl et al.[57] and Fieweger et al.[58] clearly show the presence of inhomogeneous flame kernels in certain tests prior to the blast wave-induced pressure spikes. This predetonative deflagration phase is evident in the CH emission traces, but is only accompanied by a noticeable pressure increase for certain fuels and conditions. It was concluded that, as long as the deflagration does not produce a significant pressure rise, the time of arrival of the detonation wave corresponds to the ignition time obtained by assuming a spatially homogeneous reaction zone.[53–58]

For most mixtures and conditions herein, the visible emission measurements showed no sign of significant predetonation deflagration, and the pressure traces demonstrated no significant pressure increase prior to arrival of the blast/detonation structure (see Fig. 1a). Hence, the assumption herein is that the ignition delay times correspond to a homogeneous reaction starting at the endwall (although the possibility of inhomogenieties influencing the ignition process cannot be completely ruled out).

Unfortunately, the moving blast wave affects the interpretation of τ_{ign} measurements when they are conducted from a sidewall location. An x-t diagram of the strong ignition process is given in Fig. 2. Ignition occurs first near the endwall at time t_D after shock-wave reflection, whereupon the blast wave travels at speed V_{ign} away from the endwall and passes the measurement location at time t_F. The true ignition delay time (relative to the endwall) can be calculated using

$$\tau_{ign} = t_D - t_B = (t_F - t_C) + l(1/V_R - 1/V_{ign}) \qquad (1)$$

where l is the distance from the endwall to the measurement location, V_R is the reflected-shock velocity, V_{ign} is the blast-wave velocity, and the times are as defined in Fig. 1. Note that the first term on the right-hand side ($t_F - t_C$), is the ignition delay time with respect to the test port, while the second term is the gasdynamic correction back to the endwall. The times t_F and t_C are taken directly from the pressure trace, and V_{ign} is assumed to be either the CJ speed (V_{CJ}) of the postshock gases (for most mixtures) or an intermediate speed between V_{CJ} and

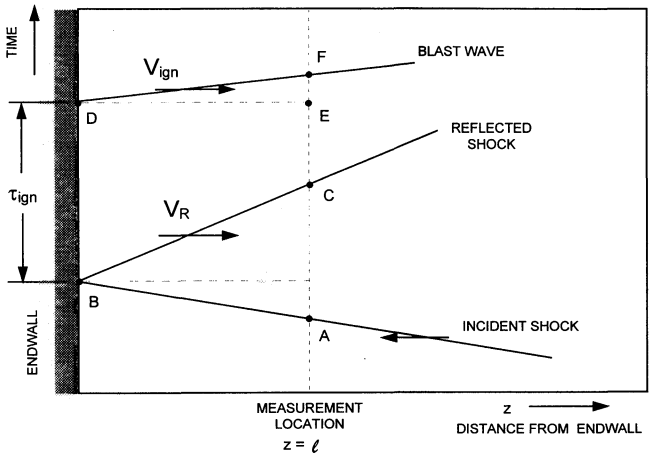

Fig. 2 Schematic (x-t) diagram illustrating the formation and propagation of a blast wave starting at the endwall. The ignition delay time is relative to the endwall ($t_D - t_B$).

the local speed of sound, a_5 (for the N_2-based mixture 2). Separate measurements were performed using a pressure transducer in both the endwall and sidewall (l = 10 mm) to confirm the blast wave correction procedure.

Approximately 30% of the ignition measurements were performed at the endwall, and so 70% of the measurements were obtained exclusively from the sidewall. Because the majority of the ignition measurements were performed at the l = 20-mm position, the typical blast wave correction was on the order of 20–45 μs, depending on the composition of the mixture. The accuracy of the correction at l = 20 mm was estimated at ± 5 μs.[34] When overlapping endwall and corrected-sidewall data were available, good agreement between the sidewall and endwall measurements was seen, supporting the use of Eq. (1) to correct the sidewall values. Further discussion on the experimental results is provided in Petersen.[34]

Given the inherent inaccuracies in 1) obtaining ignition delay times in general, 2) defining time zero caused by bifurcation of the reflected shock wave, and 3) assuming a certain V_{ign} for the blast wave correction, the overall uncertainty in τ_{ign} is estimated at ± 10 μs.

Experimental Results

A listing of all τ_{ign} data is provided in Table 2. The results in Table 2 are grouped by mixture and similar pressure and contain the τ_{ign} derived via both pressure and emission diagnostics. Next are the analyses and interpretations of each mixture and the resulting ignition delay time correlations.

Baseline Mixtures

Ignition delay times of the standard ARL mixture ($3CH_4 + 2O_2 + 10X$, X = N_2, Ar), i.e., mixtures 2 and 3 of Table 1, were measured over a range of temperatures from 1175 to 1540 K and pressures between 35 and 260 atm. These temperatures and pressures are representative of ram accelerator forebody conditions under realistic fill pressures. Because the $3CH_4 + 2O_2 + 10N_2$ (mixture 3) combination is the baseline against which the ARL propellant combinations are compared, more experiments were devoted toward its characterization than to the other Table 1 mixtures. Typical pressure and emission traces for the baseline mixtures are provided in Figs. 1a and 1b. By comparing the available emission data with the pressure information, no preignition deflagration was observed for the baseline mixtures. Figure 3a contains the experimental τ_{ign} results. Slight pressure adjustments, using the correlated dependence described next, were made to better display the data on lines of constant pressure.

Three conclusions are evident from the Fig. 3a ignition-time plot. First, the ignition delay times decrease with increasing pressure, as expected. Second, there is no discernible difference between the N_2- and Ar-based results. This observation implies the baseline ignition times may be independent of the diluent gas type. Similar results were observed in previous shock-tube studies of methane ignition.[22,59,60] Finally, the slope at lower temperatures is noticeably different from the slope at elevated temperatures. The observed shift occurs at higher temperatures as the pressure increases per the approximate relation: $T_{tr} = 1266 + 0.29P$, with the transition temperature, T_{tr}, in K and the pressure, P, in atm. For example, the transition is near 1290 K at 85 atm and 1315 K at 170 atm.

All of the baseline-mixture data of Fig. 3a could be correlated using an Arrhenius expression of the form

$$\tau_{ign} = A[M]^x \exp(E/RT) \tag{2}$$

where τ_{ign} is the ignition delay time in seconds; $[M]$ is the total concentration in mol/cm^3, i.e., P/RT; E is an activation energy in kcal/mol; R is the universal gas constant {0.001987 kcal/mol-K in Eq. (2), 82.06 cm^3-atm/mol-K in $[M]$}; and T is the temperature in K. Separate correlations were required for the high- and low-temperature regions. The Eq. (2) constants are provided in Table 1, and the results are displayed in Fig. 3b. As seen in Fig. 3b, the correlations are very good, with the high-temperature fit having a statistical regression coefficient, r^2, of 0.982. The low-temperature fit has r^2 = 0.986.

Comparisons between the two temperature regimes stress differences between the pressure dependence and the activation energy. The pressure dependence comes from the exponent of $[M]$, where the high-temperature data are proportional to $P^{-1.23}$ and the low-temperature data vary as $P^{-1.67}$. As evident from the data in Fig. 3a, the activation energy at higher ram accelerator temperatures (40.6 kcal/mol) is a factor of 2 larger than at lower temperatures (19.4 kcal/mol). Such a shift in temperature dependence can have drastic effects on predicted ignition times if the high-temperature correlation is mistakenly extrapolated below the transition temperature. For example, at 100 atm and 1150 K, the baseline ignition delay time should be 590 μs; if the high-temperature relation were used, a time of 1.8 ms would be predicted, a factor of 3 too high. Knowledge of the temperature/ignition-time relationship in both temperature zones is crucial for the ram accelerator because the expected forebody ignition temperature (<1400 K)[12] can fall in either regime.

High-Concentration Mixtures

The high-concentration mixtures ($3CH_4 + 2O_2 + 6X$, X = N_2, Ar), i.e., mixtures 4 and 5 in Table 1, have the same stoichiometry (ϕ = 3.0) as the baseline mixtures, but a higher concentration of fuel and oxidizer and, therefore, less diluent. Temperatures between 1040 and 1370 K and pressures from 45 to 190 atm were considered. No mixture 4 or 5 experiment displayed any visible emission or pressure increase prior to t_F, indicating the absence of a significant inhomogeneous deflagration phase prior to strong ignition.

Presented in the Fig. 4a Arrhenius diagram are the τ_{ign} results for mixtures 4 and 5; the complete listings are provided in Table 2. As seen in the baseline results, the high-concentration data in Fig. 4a show a distinct slope change between the high- and low-temperature regions. The transition temperature varies approximately with pressure as $T_{tr} = 1216 + 0.42P$.

Figure 4b displays the correlated ignition time data in the form of Eq. (2), and Table 1 lists the best-fit correlation parameters. The regression coefficients for the high- and low-temperature relations are 0.993 and 0.981, respectively. In general, the results and trends are similar to those observed for the baseline mixtures. The high-temperature activation energy (30.6 kcal/mol), however, is lower than the analogous high-temperature baseline activation energy (40.6 kcal/mol), most likely because of the lower range of temperatures tested for mixtures 4 and 5.

Table 2 Experimental ignition delay time data

Mixture	P, atm	T, K	τ_{ign},[a] μs	τ_{emis},[b] μs
1	50			
	50.5, 50, 49,	1203, 1232, 1268,	694, 555, 406,	689 (236[c]), 565 (189[c]), ——,
	44.4, 48.9, 47.3	1285, 1319, 1359	415, 261, 206	407 (171[c]), 273 (130[c]), 202 (115[c])
1	100			
	100.9, 98.8, 96.2, 94.7,	1137, 1169, 1198, 1207,	661, 541, 440, 392,	——, 532 (200[c]), ——, ——,
	98.2, 100, 94.5, 94.7	1268, 1292, 1312, 1361	241, 191, 169, 114	239 (96[c]), 188 (98[c]), 161, 108
1	150			
	161.2, 150.8	1198, 1250	253, 177	244 (107[c]), 175 (95[c])
2	40			
	39.8, 47.5, 38.4,	1325, 1346, 1383,	654, 361,[d] 391,	——, ——, ——,
	34.5, 35.6	1431, 1536	250, 102	——, ——
2	85			
	91, 80.9, 77.7,	1167, 1196, 1203,	572, 681,[d] 622,	563, ——, 607,
	83, 91.8, 92.9	1206, 1363, 1418	541, 152,[d] 95[d]	541, ——, ——
2	115			
	106, 132.2, 102.8,	1179, 1182, 1182,	414, 280, 419,	415, 274, 419,
	114, 114.4, 120	1156, 1244, 1380	421, 254, 77	430, 260, 71
2	170			
	178.4, 163, 164	1209, 1254, 1372	170, 157, 71	——, ——, ——
2	260			
	262.5, 263.6, 256.2	1176, 1239, 1301	98, 70, 55	——, ——, ——
3	40			
	47.3, 41.4, 36.7, 43.3, 48.2,	1358, 1362, 1381, 1402, 1409,	327, 360, 425, 265, 214,	——, ——, ——, ——, ——,
	42.2, 40.4, 39.5, 44.3, 39.3	1414, 1418, 1454, 1486, 1511	238, 234, 182, 115, 106	——, ——, ——, ——, ——
3	75			
	72.1, 76.1, 74,	1290, 1334, 1366,	431, 259, 194,	416,[e] ——, ——,
	76.5, 75.7	1408, 1466	124, 74	112,[e] 74[e]
3	85			
	92, 86.9, 84.1,	1227, 1273, 1316,	504,[d] 445,[d] 330,[d]	508, 468, 344,
	85, 84.4	1390, 1437	152,[d] 80[d]	163, 86
3	115			
	113, 116.8,	1149, 1238,	533,[d] 282,[d]	537, ——,
	103.1, 117.4	1286, 1323	233,[d] 155[d]	——, ——
3	140			
	145, 139.6,	1186, 1216,	261,[d] 227,[d]	——, ——,
	148.2, 134.9	1293, 1317	130,[d] 135[d]	——, ——
4	50			
	51.5, 46.6, 44.9	1191, 1265, 1362	847, 530, 221	854, 530, 230
4	65			
	71.3, 64.3, 60.4	1215, 1283, 1346	411,[d] 288,[d] 190[d]	——, ——, ——
4	130			
	125.5, 128	1089, 1156	331, 231	338, 231
5	55			
	55.3, 54.4, 59.6	1196, 1258, 1371	738, 453, 151	742, 453,[f] ——
5	85			
	86.6, 82.8	1242, 1272	228, 200	232,[f] 195[f]
5	130			
	128.4, 139.9, 138.5, 122.8,	1041, 1138, 1186, 1249,	433,[d] 194,[d] 182,[d] 142,[d]	——, ——, 186, ——,
	133, 136, 129.7	1250, 1304, 1327	118,[d] 89,[d] 81[d]	——, ——, ——
5	180			
	176.6, 188.7,	1150, 1230,	120, 71,	111,[f] ——,
	194, 169.7	1235, 1268	67, 72	——, ——
6	15			
	20.3, 13.8, 18.6,	1453, 1520, 1523,	466,[g] 420,[g] 333,[g]	——, ——, ——,
	13.8, 15.2, 12	1529, 1548, 1607	391,[g] 345,[g] 265[g]	——, ——, ——
6	55			
	57.2, 51.2	1456, 1547	86, 58	82, 58
6	70			
	79, 72.8, 68.4	1324, 1367, 1395	185, 135, 111	187, 138, 105
6	90			
	90.7, 91.3, 81.6	1128, 1203, 1290	332, 315, 249	334, 297, 241
7	30			
	35.5, 29.5,	1272, 1338,	875, 591,	——, 651 (557[c]),
	28.9, 27	1398, 1458	418, 260	425, 269
7	50			
	49.5, 47.1	1342, 1469	379, 149	399, 151 (44[c])
7	60			
	57.2, 61.5, 60.5	1296, 1366, 1391	529, 181,[d] 152[d]	572, 180, 151
7	75			
	76.4	1347	233	233
7	100			
	92.5, 106.6	1340, 1358	128, 111	128, 111

[a]Based on sidewall pressure measurement, unless otherwise noted. [b]Based on visible emission (Si photodiode), unless otherwise noted. [c]Onset of deflagration. [d]Endwall pressure measurement. [e]CH_4 emission (3.3 μm). [f]CH emission (431 nm). [g]HeNe laser extinction measurement.

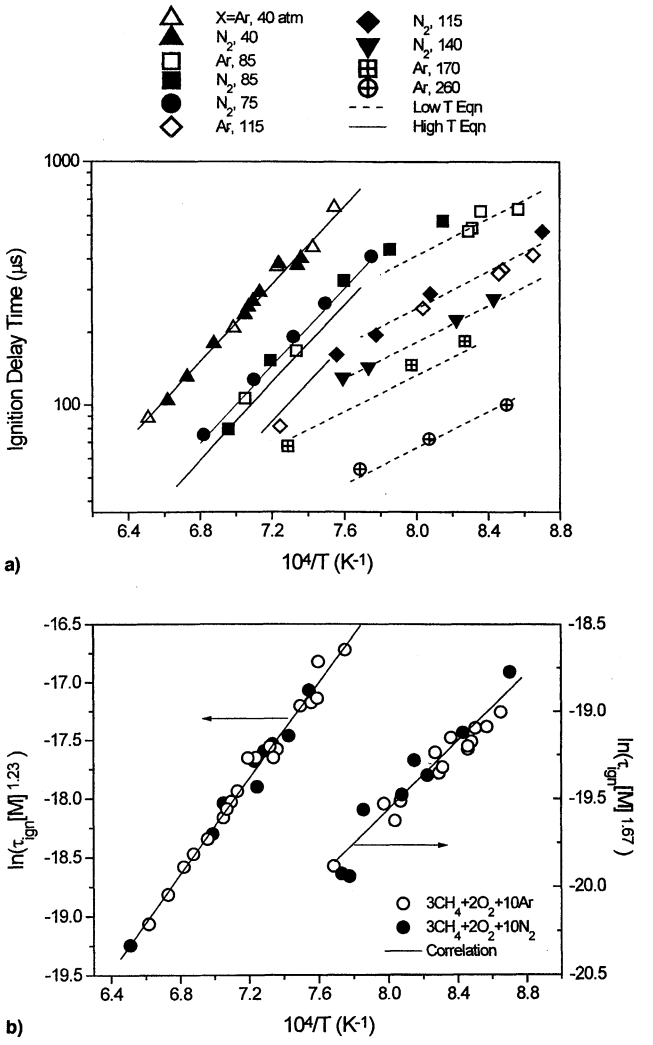

Fig. 3 Baseline mixture results ($3CH_4 + 2O_2 + 10X$; X = N_2, Ar): a) baseline mixture ignition delay times and b) baseline mixture correlations. Left axis: high-temperature correlation (r^2 = 0.982); right axis: low-temperature correlation (r^2 = 0.986).

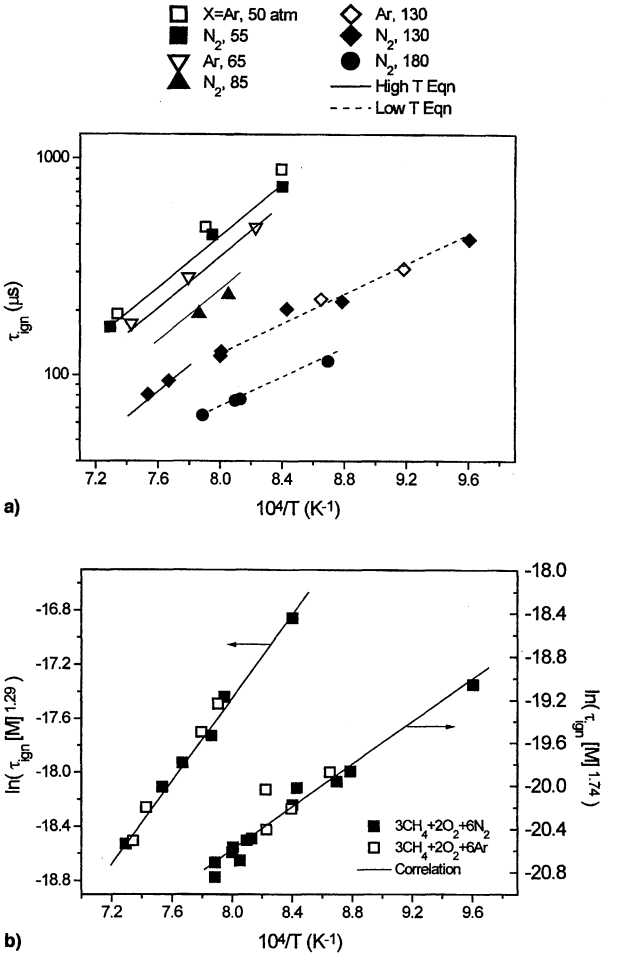

Fig. 4 High-concentration mixture results ($3CH_4 + 2O_2 + 6X$; X = N_2, Ar): a) high-concentration mixture ignition delay times and b) high-concentration mixture correlations. Left axis: high-temperature correlation (r^2 = 0.993); right axis: low-temperature correlation (r^2 = 0.981).

Helium-Based Mixture

A limited number of measurements were performed with the $6CH_4 + 2O_2 + 4He$ mixture (mixture 6, Table 1). This propellant combination differs from the baseline case in its stoichiometry (ϕ = 6.0), bath gas (helium), and higher concentration of fuel and oxidizer. The comparatively low molecular weight of the helium-based mixture limited the achievable shock-tube test pressure and test time. Nevertheless, pressures from 12 to 90 atm and temperatures between 1130 and 1600 K were attained. No preignition emission was evident in the helium-based tests, indicating no significant deflagration phase prior to t_F.

Most data fell into the high-temperature ignition regime, although two points were clearly in the low-temperature zone. Figure 5 presents the subsequent correlation of the higher temperature data (r^2 = 0.983). Table 1 contains the correlation parameters. The resulting pressure dependence ($P^{-1.46}$) and activation energy (37.5 kcal/mol) are similar to the other fuel-rich mixtures in Table 1.

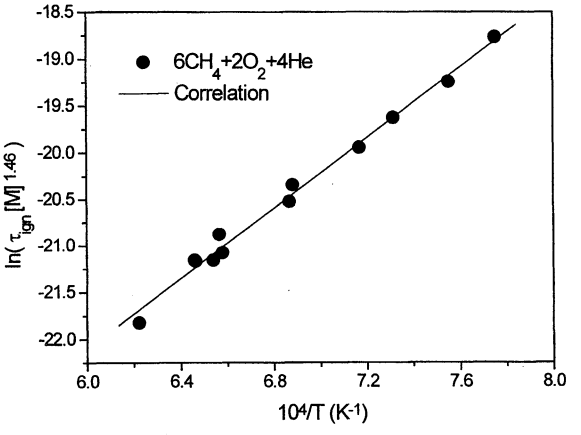

Fig. 5 Helium-based mixture ($6CH_4 + 2O_2 + 4He$) ignition delay times and high-temperature correlation (r^2 = 0.983).

Helium–Nitrogen Mixture

Twelve experiments were performed with mixture 7, which contained a combination of both N_2 and He as the diluent, i.e., $3CH_4 + 2O_2 + 4N_2 + 8He$. The data for this mixture fell exclusively in the higher temperature regime, covering temperatures from 1272 to 1469 K and pressures from 27 to 107 atm. Table 2 lists the individual data points.

Although the occurrence of strong ignition was evident in all pressure traces, some visible emission traces displayed a slight increase prior to arrival of the detonation/blast wave, signifying a mild deflagration phase.[58] However, the pressure exhibited only a slight, if any, increase prior to time t_F. Therefore, τ_{ign} was assumed to correspond with the arrival of the blast wave per a homogeneous reaction assumption, as in Pfahl

et al.[57] and Fieweger et al.,[58] for high-pressure hydrocarbon ignition.

The mixture 7 ignition delay time data were well-correlated per Eq. (2) with the constants provided in Table 1. A −1.22 pressure dependence and a 34.4-kcal/mol activation energy resulted. The correlated data are displayed in Fig. 6 ($r^2 = 0.953$). Because no experiments below 1272 K were performed, a low-temperature correlation was not obtained for the He–N_2 mixture.

Fuel-Lean Mixture

A total of 16 experiments were performed to determine the ignition delay time characteristics of the $0.4CH_4 + 2O_2 + 8Ar$ mixture (mixture 1, Table 1). Temperatures between 1135 and 1360 K and pressures from 44 to 160 atm were covered. Typical pressure and emission data are shown in Fig. 7, wherein weak ignition is evident in the fuel-lean emission trace prior to arrival of the detonation wave. This deflagration phase begins at time τ_{defl}, as defined in Fig. 7, and was evident for most mixture 1 experiments that utilized the emission diagnostic. However, no significant pressure increase was observed during any of the deflagration phases, so that τ_{ign} was defined for each mixture 1 measurement as the time of arrival of the blast wave at the test port, per Eq. (1) and Fig. 7, i.e., at time t_F.

The ignition-time results are displayed in the Arrhenius plot of Fig. 8a. Unlike the fuel-rich mixtures presented earlier, the fuel-lean results did not show a change in temperature dependence at lower temperatures (for the range of conditions studied). A single correlation of the ignition delay times for the entire range of temperatures (1135–1360 K) is given in Table 1 and has an overall activation energy of 27.8 kcal/mol and a

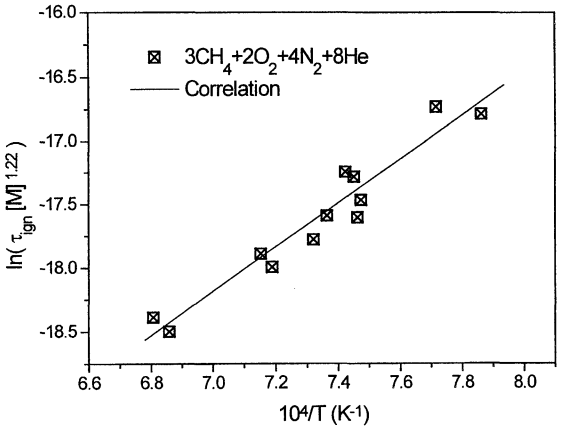

Fig. 6 He-N_2-based mixture ($3CH_4 + 2O_2 + 4N_2 + 8He$) ignition delay times and high-temperature correlation ($r^2 = 0.953$).

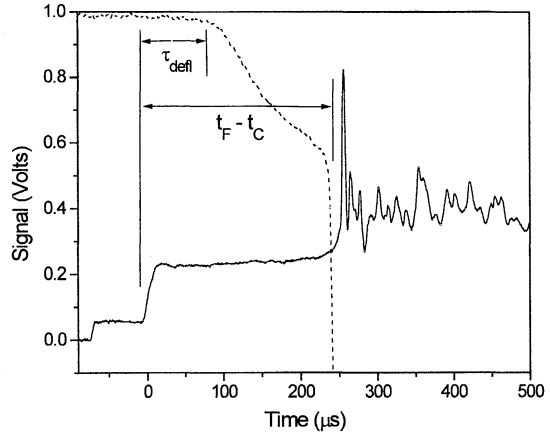

Fig. 7 Typical pressure and visible emission data for the fuel-lean mixture (mixture 1, Table 1). A deflagration phase is evident in the emission trace; 1319 K, 49 atm.

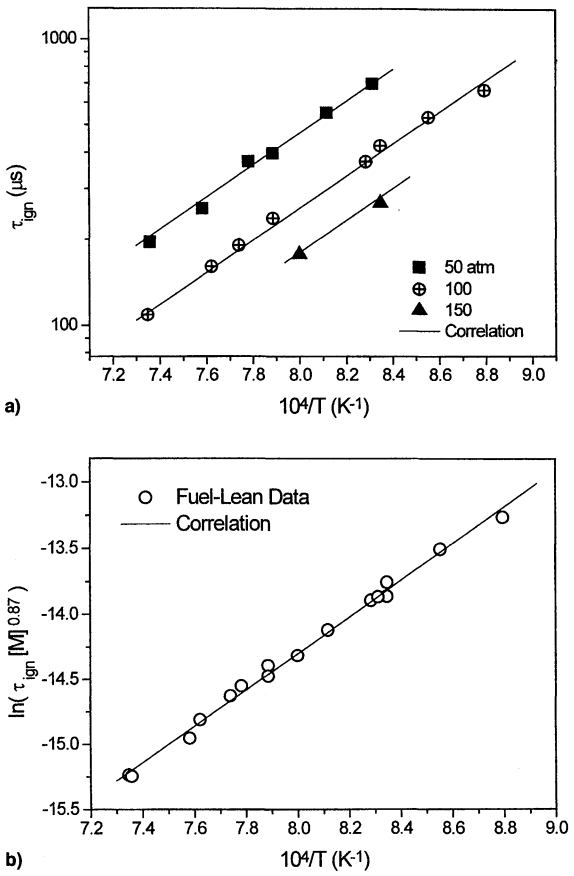

Fig. 8 Fuel-lean mixture results ($0.4CH_4 + 2O_2 + 8Ar$): a) fuel-lean ignition delay times and b) fuel-lean mixture correlation ($r^2 = 0.994$).

pressure dependence of only −0.87. The coefficient of multiple determination r^2 is greater than 0.99. Figure 8b displays the correlated data.

Discussion

A comparison of the ignition delay times for each mixture results in the observation that the baseline (mixture 3), fuel-lean (mixture 1), and He–N_2-based (mixture 7) mixtures produced ignition delay times that are nearly a factor of 2 longer than the τ_{ign} obtained for the less-dilute mixtures, i.e., mixtures 4–6. Of more general utility, though, is the fact that the entire data set can be well correlated by two expressions, one for each temperature regime. Such relations are useful for extrapolation to other propellant combinations. The subsequent high-temperature correlation ($r^2 = 0.948$) is

$$\tau_{ign} = 1.26 \times 10^{-14}[CH_4]^{-0.02}[O_2]^{-1.20} \exp(32{,}700/RT) \quad (3)$$

and the corresponding low-temperature expression ($r^2 = 0.982$) is

$$\tau_{ign} = 4.99 \times 10^{-14}[CH_4]^{-0.38}[O_2]^{-1.31} \exp(18{,}950/RT) \quad (4)$$

The empirical transition temperature between the two regimes is given approximately by

$$T_{tr} = 1347 + 0.34P - 665X_{O_2} \quad (5)$$

In the preceding equations, τ_{ign} is the ignition delay time in seconds, [A] is the concentration of species A in mol/cm^3, R is the universal gas constant in cal/mol-K, P is the pressure in atm, X_{O_2} is the oxygen mole fraction, and the temperatures (T, T_{tr}) are in Kelvin. Equation (4) comprises all of the lower

temperature data except for those obtained with the fuel-lean mixture. Attempts to correlate the low-temperature (<1300 K), fuel-lean data with the low-temperature, fuel-rich data were not successful, indicating the chemistry of the fuel-lean mixture differs from that of the fuel-rich ones at lower temperatures. This result is not surprising, as no accelerated temperature dependence was observed for mixture 1 (Fig. 8a). The lower temperature mixture 1 data are included in the higher temperature correlation of Eq. (3).

Figure 9 displays the overall data correlations. As shown, most ignition times are represented by Eqs. (3) and (4) to better than 25%. The high-temperature correlation [Eq. (3)], is virtually independent of the amount of methane present, and the overall pressure dependence of Eqs. (3) and (4) are the same as the individual mixture correlations in Table 1 (≈ -1.2 and -1.7, respectively). Also evident in Eqs. (3) and (4) and Fig. 9 is the relative insensitivity of the measured ignition delay time to the type and amount of diluent for the entire range of gases and conditions considered. Equations (3) and (4) are intended for τ_{ign} estimates of mixtures not tested herein; i.e., the individual correlations [Eq. (2), Table 1] should still be utilized when estimating ignition delay times for the Table 1 mixtures.

Equation (5) is based on only eight T_{tr} data points from Figs. 3a and 4a, and the oxygen mole fraction term incorporates the single T_{tr} point from the $3CH_4 + 2O_2 + 4He$ data; extrapolation of this simple relation much beyond an equivalence ratio of 3.0 is cautioned. However, the actual transition between the low- and high-temperature regimes is in fact more gradual than suggested by the T_{tr} of Eq. (5). Most important, however, is the range of temperatures in which to expect the transition. For the mixture compositions and pressures (50–250 atm) of interest, the transition temperature resides between 1240 and 1340 K.

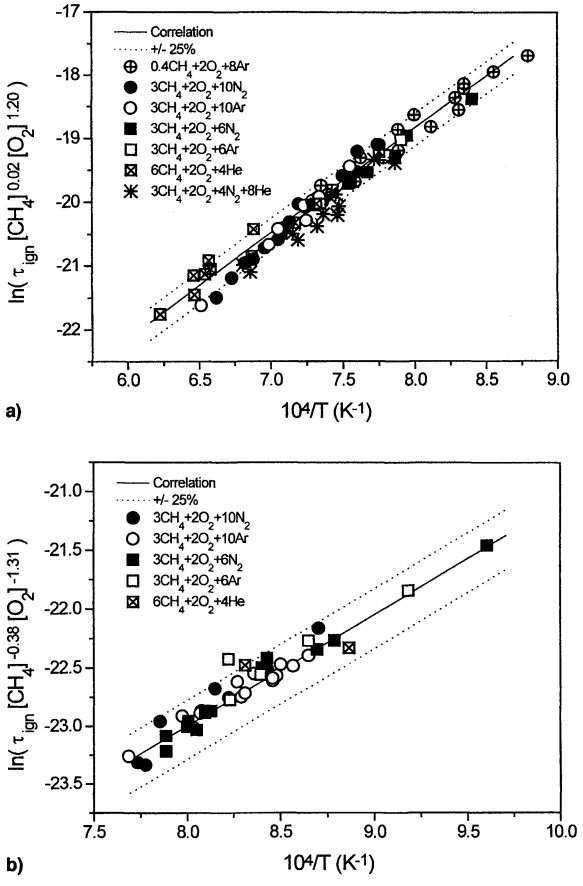

Fig. 9 Overall ignition delay time correlations: a) high-temperature correlation ($r^2 = 0.948$) and b) low-temperature correlation ($r^2 = 0.982$).

Perhaps the most significant observation in the present study is the sudden change in the temperature dependence of τ_{ign} at low temperatures and high pressures (Figs. 3, 4, and 9). A similar shift is routinely seen in higher-order hydrocarbons (C_{3+}) under engine-like conditions.[54,61] A few studies demonstrating low-temperature τ_{ign} transitions in smaller hydrocarbons were found in the literature. Skinner and Ruehrwein[62] report 6-atm, $\phi = 3$ methane ignition time data in tabular form that contain a transition near 1250 K, but no mention of it was made in their paper. Asaba et al.[63] present $\phi = 2$, CH_4/O_2 ignition delay times at 7 atm that clearly display a transition between 1250 and 1400 K, but they incorrectly attribute the deviation to data scatter. The low-temperature, $C_2H_4/O_2/Ar$ shock-tube data of Suzuki et al.[64] show a similar change in slope near 1100 K for stoichiometries ranging from fuel-lean to fuel-rich. Finally, the low-pressure propane oxidation data of Myers and Bartle[65] have distinct transitions near 1250 K for $\phi = 0.1-1.5$. No explanation of the transition zone kinetics was provided in these papers.

Because hydrocarbon ignition is primarily a chain-branching phenomenon,[19,61] a shift in the ignition time characteristics must indicate a change in the chain branching and propagation pathways. In a companion analytical study, the authors present a detailed chemical kinetics model for high-pressure, fuel-rich, intermediate-temperature CH_4/O_2 ignition that successfully reproduces the decreased temperature dependence at the lower temperatures.[66] The reader should therefore consult Refs. 34 and 66 for further discussions on high-pressure CH_4/O_2 chemical kinetics and ignition.

During the fuel-rich experiments, an interesting soot-formation phenomenon was observed. At the lowest pressures and highest temperatures, large soot deposits were found in the shock tube after a visual, posttest inspection. This result was not unexpected, however, given the high CH_4 concentrations utilized. On the other hand, after the highest-pressure and lowest-temperature experiments, a liquid hydrocarbon residue was found in the shock tube instead of soot. These results were highly repeatable for a given mixture and test conditions. Although no further investigations were performed on this matter, the experimental records indicate that the demarcation between soot and liquid formation corresponds roughly with the activation energy transition seen in Figs. 3a and 4a. High-pressure soot and aromatic hydrocarbon formation in shock tubes remains a topic for future study.

Conclusions

Ignition delay times were measured for the following ram accelerator mixtures: $3CH_4 + 2O_2 + 10X$, $3CH_4 + 2O_2 + 6X$, $6CH_4 + 2O_2 + 4He$, $3CH_4 + 2O_2 + 4N_2 + 8He$, and $0.4CH_4 + 2O_2 + 8Ar$, where $X = N_2$ or Ar. All experiments were performed behind reflected shock waves in a high-pressure shock tube. Temperatures and pressures important to ram accelerator forebody ignition were explored (1040–1600 K, 35–260 atm), and ignition time correlations were generated for each mixture. A correlation of the entire data set was also obtained. These results led to the conclusion that ignition delay time is not a strong function of the amount or type of diluent.

The ignition kinetics at low temperatures and high pressures were such that a distinct transition in the temperature dependence was observed for the fuel-rich mixtures. The transition temperature for the stoichiometries and pressures investigated was between 1240 and 1340 K (the region of prime interest to ram accelerator ignition). Similar characteristics are commonly observed in higher-order hydrocarbons where the transition occurs because of competition between high- and low-temperature chain branching.

Acknowledgments

This work was supported by the U.S. Army Research Office, with David Mann as the Program Monitor, and the Office of Naval Research, with Richard Miller as the Program Monitor.

Interaction with Michael J. Nusca of the U.S. Army Research Laboratory proved helpful throughout the investigation, and discussions with C. T. Bowman and Ulrich Pfahl were invaluable. The assistance of Michael Röhrig and Ronald W. Bates in the laboratory is appreciated.

References

[1]Hertzberg, A., Bruckner, A. P., and Bogdanoff, D. W., "Ram Accelerator: A New Chemical Method for Accelerating Projectiles to Ultrahigh Velocities," *AIAA Journal*, Vol. 26, No. 2, 1988, pp. 195–203.

[2]Bruckner, A. P., Knowlen, C., Hertzberg, A., and Bogdanoff, D. W., "Operational Characteristics of the Thermally Choked Ram Accelerator," *Journal of Propulsion and Power*, Vol. 7, No. 5, 1991, pp. 828–836.

[3]Zhang, F., Frost, D. L., Chue, R. S., Lee, J. H. S., Thibault, P., and Yee, C., "Stability Studies of Detonation Driven Projectiles," *Shock Waves @ Marseille I, Proceedings of the 19th International Symposium on Shock Waves*, edited by R. Brun and L. Z. Dumitrescu, Springer–Verlag, Berlin, 1995, pp. 177–182.

[4]Soetrisno, M., Imlay, S. T., and Roberts, D. W., "Numerical Simulations of the Superdetonative Ram Accelerator Combusting Flow Field," AIAA Paper 93-2185, June 1993.

[5]Kruczynski, D. L., and Liberatore, F., "Ram Accelerator Experiments with Unique Projectile Geometries," AIAA Paper 95-2490, July 1995.

[6]Hinkey, J. B., Burnham, E. A., and Bruckner, A. P., "High Spatial Resolution Measurements of Ram Accelerator Gas Dynamic Phenomena," AIAA Paper 92-3244, July 1992.

[7]Higgins, A. J., Knowlen, C., and Bruckner, A. P., "An Investigation of Ram Accelerator Gas Dynamic Limits," AIAA Paper 93-2181, June 1993.

[8]Hertzberg, A., Bruckner, A. P., and Knowlen, C., "Experimental Investigation of Ram Accelerator Propulsion Modes," *Shock Waves*, Vol. 1, 1991, pp. 17–25.

[9]Kruczynski, D. L., "New Experiments in a 120-mm Ram Accelerator at High Pressures," AIAA Paper 93-2589, June 1993.

[10]Kruczynski, D. L., and Liberatore, F., "Experimental Investigation of High Pressure/Performance Ram Accelerator Operation," AIAA Paper 96-2676, July 1996.

[11]Nusca, M. J., "Investigation of Ram Accelerator Flows for High Pressure Mixtures of Various Chemical Compositions," AIAA Paper 96-2946, July 1996.

[12]Nusca, M. J., and Kruczynski, D. L., "Reacting Flow Simulation for a Large-Scale Ram Accelerator," *Journal of Propulsion and Power*, Vol. 12, No. 1, 1996, pp. 61–69.

[13]Knowlen, C., Higgins, A. J., Bruckner, A. P., and Hertzberg, A., "In-Tube Photography of Ram Accelerator Projectiles," *Shock Waves @ Marseille I, Proceedings of the 19th International Symposium on Shock Waves*, edited by R. Brun and L. Z. Dumitrescu, Springer–Verlag, Berlin, 1995, pp. 189–194.

[14]Kruczynski, D. L., Liberatore, F., and Kiwan, M., "Flow Visualization of Steady and Transient Combustion in a 120-mm Ram Accelerator," AIAA Paper 94-3344, June 1994.

[15]Yungster, S., and Bruckner, A. P., "Computational Studies of a Superdetonative Ram Accelerator Mode," *Journal of Propulsion and Power*, Vol. 8, No. 2, 1992, pp. 457–463.

[16]Nusca, M. J., "Computational Simulation of the Ram Accelerator Using a Coupled CFD/Interior-Ballistics Approach," AIAA Paper 97-2653, July 1997.

[17]Dyne, B. R., and Heinrich, J. C., "Finite Element Analysis of the Scramaccelerator with Hydrogen-Oxygen Combustion," *Journal of Propulsion and Power*, Vol. 12, No. 2, 1996, pp. 336–340.

[18]Li, C., Kailasanath, K., Oran, E. S., Landsberg, A. M., and Boris, J. P., "Dynamics of Oblique Detonations in Ram Accelerators," *Shock Waves*, Vol. 5, No. 1/2, 1995, pp. 97–101.

[19]Westbrook, C. K., and Dryer, F. L., "Chemical Kinetic Modeling of Hydrocarbon Combustion," *Progress in Energy and Combustion Science*, Vol. 10, 1984, pp. 1–57.

[20]Dagaut, P., Boettner, J.-C., and Cathonnet, M., "Methane Oxidation: Experimental and Kinetic Modeling Study," *Combustion Science and Technology*, Vol. 77, Nos. 1–3, 1991, pp. 127–148.

[21]Spadaccini, L., and Colket, M., III, "Ignition Delay Characteristics of Methane Fuels," *Progress in Energy and Combustion Science*, Vol. 20, 1994, pp. 431–460.

[22]Petersen, E. L., Röhrig, M., Davidson, D. F., Hanson, R. K., and Bowman, C. T., "High-Pressure Methane Oxidation Behind Reflected Shock Waves," *26th Symposium (International) on Combustion*, The Combustion Inst., Pittsburgh, PA, 1996, pp. 799–806.

[23]Frenklach, M., Wang, H., Goldenberg, M., Smith, G. P., Golden, D. M., Bowman, C. T., Hanson, R. K., Gardiner, W. C., and Lissianski, V., "GRI-Mech—An Optimized Detailed Chemical Reaction Mechanism for Methane Combustion," Gas Research Institute Topical, Rept. GRI-95/0058, 1995.

[24]Anderson, W. R., and Kotlar, A. J., "Detailed Modeling of CH_4/O_2 Combustion for Hybrid In-Bore Ram Propulsion (HIRAM) Application," *1990 JANNAF Combustion Subcommittee Meeting*, Vol. 2, 1991, pp. 417–426 (CPIA Pub. 573).

[25]Petersen, E. L., Davidson, D. F., and Hanson, R. K., "Ignition Delay Times of Ram Accelerator Mixtures," AIAA Paper 96-2681, July 1996.

[26]Petersen, E. L., Davidson, D. F., and Hanson, R. K., "Ram Accelerator Mixture Chemistry: Kinetics Modeling and Ignition Measurements," *1996 JANNAF Combustion Subcommittee Meeting*, Vol. 1, 1997, pp. 395–407 (CPIA Pub. 653).

[27]Petersen, E. L., Davidson, D. F., Röhrig, M., and Hanson, R. K., "High-Pressure Shock Tube Measurements of Ignition Times in Stoichiometric $H_2/O_2/Ar$ mixtures," *Shock Waves—Proceedings of the 20th International Symposium on Shock Waves*, edited by B. Sturtevant, J. E. Shephard, and H. G. Hornung, World Scientific, River Edge, NJ, 1996, pp. 941–946.

[28]Kruczynski, D. L., and Liberatore, F., "Ram Accelerator Experiments with Unique Projectile Geometries," AIAA Paper 95-2490, July 1995.

[29]Crossley, R. W., Dorko, E. A., Scheller, K., and Burcat, A., "The Effect of Higher Alkanes on the Ignition of Methane-Oxygen-Argon Mixtures in Shock Tubes," *Combustion and Flame*, Vol. 19, 1972, pp. 373–378.

[30]Schmitt, R. G., and Butler, P. B., "Detonation Properties of Gases at Elevated Initial Pressures," *Combustion Science and Technology*, Vol. 106, 1995, pp. 167–191.

[31]Davidson, D. F., and Hanson, R. K., "Real Gas Corrections in Shock Tube Studies at High Pressures," *Israeli Journal of Chemistry*, Vol. 36, 1996, pp. 321–326.

[32]Davidson, D. F., Bates, R. W., Petersen, E. L., and Hanson, R. K., Shock Tube Measurements of the Equation of State of Argon," AIAA Paper 97-0984, Jan. 1997; also 13th Symposium on Thermophysical Properties, Boulder, CO, June 1997.

[33]Mirels, H., and Braun, W. H., "Nonuniformities in Shock-Tube Flow Due to Unsteady-Boundary-Layer Action," NACA TN 4021, May 1957.

[34]Petersen, E. L., "A Shock Tube and Diagnostics for Chemistry Measurements at Elevated Pressures with Application to Methane Ignition," Ph.D. Dissertation, Dept. of Mechanical Engineering, Stanford Univ., Stanford, CA, March 1998.

[35]Mark, H., "The Interaction of a Reflected Shock Wave with the Boundary Layer in a Shock Tube," NACA TM 1418, March 1958.

[36]Petersen, E. L., and Hanson, R. K., "Measurements of Reflected-Shock Bifurcation in a High-Pressure Shock Tube," *Shock Waves* (submitted for publication).

[37]Voevodsky, V. V., and Soloukhin, R. I., "On the Mechanism and Explosion Limits of Hydrogen-Oxygen Chain Self-Ignition in Shock Waves," *10th Symposium (International) on Combustion*, The Combustion Inst., Pittsburgh, PA, 1965, pp. 279–283.

[38]Soloukhin, R. I., "Quasi-Stationary Reaction Zone in Gaseous Detonation," *11th Symposium (International) on Combustion*, The Combustion Institute, Pittsburgh, PA, 1967, pp. 671–676.

[39]Strehlow, R. A., and Cohen, A., "Initiation of Detonation," *Physics of Fluids*, Vol. 5, No. 1, 1962, pp. 97–101.

[40]Gilbert, R. B., and Strehlow, R. A., "Theory of Detonation Initiation Behind Reflected Shock Waves," *AIAA Journal*, Vol. 4, No. 10, 1966, pp. 1777–1783.

[41]Strehlow, R. A., Crooker, A. J., and Cusey, R. E., "Detonation Initiation Behind an Accelerating Shock Wave," *Combustion and Flame*, Vol. 11, 1967, pp. 339–350.

[42]Meyer, J. W., and Oppenheim, A. K., "Coherence Theory of the Strong Ignition Limit," *Combustion and Flame*, Vol. 17, 1971, pp. 65–68.

[43]Meyer, J. W., and Oppenheim, A. K., "On the Shock-Induced Ignition of Explosive Gases," *13th Symposium (International) on Combustion*, The Combustion Inst., Pittsburgh, PA, 1971, pp. 1153–1164.

[44]Meyer, J. W., Cohen, L. M., and Oppenheim, A. K., "Study of Exothermic Processes in Shock Ignited Gases by the Use of Laser Shear Interferometry," *Combustion Science and Technology*, Vol. 8, No. 4, 1973, pp. 185–197.

[45]Oppenheim, A. K., Cohen, L. M., Short, J. M., Cheng, R. K., and Hom, K., "Dynamics of the Exothermic Process in Combustion," *15th Symposium (International) on Combustion*, The Combustion Inst., Pittsburgh, PA, 1974, pp. 1503–1513.

[46]Vermeer, D. J., Meyer, J. W., and Oppenheim, A. K., "Auto-Ignition of Hydrocarbons Behind Reflected Shock Waves," *Combustion and Flame*, Vol. 18, 1972, pp. 327–336.

[47]Oppenheim, A. K., Cohen, L. M., Short, J. M., Cheng, R. K., and Hom, K., "Shock Tube Studies of Exothermic Processes in Combustion," *Modern Developments in Shock Tube Research, Proceedings of the 10th International Shock Tube Symposium* (Kyoto, Japan), 1975, pp. 557–568.

[48]Cheng, R. K., Short, J. M., and Oppenheim, A. K., "Diagnostics of the Exothermic Process," *Experimental Diagnostics in Gas Phase Combustion Systems*, edited by B. T. Zinn, Vol. 53, Progress in Astronautics and Aeronautics, AIAA, New York, 1976.

[49]Cheng, R. K., and Oppenheim, A. K., "Autoignition in Methane-Hydrogen Mixtures," *Combustion and Flame*, Vol. 58, No. 2, 1984, pp. 125–139.

[50]Cohen, L. M., Short, J. M., and Oppenheim, A. K., "A Computational Technique for the Evaluation of Dynamic Effects of Exothermic Reactions," *Combustion and Flame*, Vol. 24, No. 3, 1975, pp. 319–334.

[51]Oran, E. S., Young, T. R., and Boris, J. P., "Weak and Strong Ignition. I. Numerical Simulations of Shock Tube Experiments," *Combustion and Flame*, Vol. 48, 1982, pp. 135–148.

[52]Oran, E. S., and Boris, J. P., "Weak and Strong Ignition. II. Sensitivity of the Hydrogen-Oxygen System," *Combustion and Flame*, Vol. 48, 1982, pp. 149–161.

[53]Ciezki, H., and Adomeit, G., "Experimental Shock-Tube Investigation of the Ignition-Delay of *n*-Heptane-O_2-N_2-Ar Mixtures Under High Pressure," *Shock Tubes and Waves, Proceedings of the 16th International Symposium on Shock Tubes and Waves* (Aachen, Germany), 1987, pp. 481–486.

[54]Ciezki, H. K., and Adomeit, G., "Shock-Tube Investigation of Self-Ignition of *n*-Heptane-Air Mixtures Under Engine Relevant Conditions," *Combustion and Flame*, Vol. 93, No. 4, 1993, pp. 421–433.

[55]Fieweger, K, Ciezki, H., and Adomeit, G., "Comparison of Shock-Tube Ignition Characteristics of Various Fuel-Air Mixtures at High Pressures," *Shock Waves @ Marseille II, Proceedings of the 19th International Symposium on Shock Waves* (Marseille, France), Springer–Verlag, Berlin, 1993, pp. 161–166.

[56]Fieweger, K., Blumenthal, R., and Adomeit, G., "Shock-Tube Investigations on the Self-Ignition of Hydrocarbon-Air Mixtures at High Pressures," *25th Symposium (International) on Combustion*, The Combustion Inst., Pittsburgh, PA, 1994, p. 1579.

[57]Pfahl, U., Fieweger, K., and Adomeit, G., "Self-Ignition of Diesel-Relevant Hydrocarbon-Air Mixtures Under Engine Conditions," *26th Symposium (International) on Combustion*, The Combustion Inst., Pittsburgh, PA, 1996, pp. 781–789.

[58]Fieweger, K., Blumenthal, R., and Adomeit, G., "Self-Ignition of S.I. Engine Model Fuels: A Shock Tube Investigation at High Pressures," *Combustion and Flame*, Vol. 109, No. 4, 1997, pp. 599–619.

[59]Grillo, A., and Slack, M. W., "Shock Tube Study of Ignition Delay Times in Methane-Oxygen-Nitrogen-Argon Mixtures," *Combustion and Flame*, Vol. 27, No. 3, 1976, pp. 377–381.

[60]Seery, D. J., and Bowman, C. T., "A Shock Tube Study of Methane Oxidation," *Proceedings of the 154th Meeting of the American Chemical Society*, 1967, pp. 82–95.

[61]Chevalier, C., Pitz, W. J., Warnatz, J., Westbrook, C. K., and Melenk, H., "Hydrocarbon Ignition: Automatic Generation of Reaction Mechanisms and Applications to Modeling of Engine Knock," *24th Symposium (International) on Combustion*, The Combustion Inst., Pittsburgh, PA, 1992, pp. 93–101.

[62]Skinner, G. B., and Ruehrwein, R. A., "Shock Tube Studies on the Pyrolysis and Oxidation of Methane," *Journal of Physical Chemistry*, Vol. 63, No. 10, 1959, pp. 1736–1742.

[63]Asaba, T., Yoneda, K., Kakihara, N., and Hikita, T., "A Shock Tube Study of Ignition of Methane-Oxygen Mixtures," *9th Symposium (International) on Combustion*, Academic, New York, 1963, pp. 193–200.

[64]Suzuki, M., Moriwaki, T., Okazaki, S., Okuda, T., and Tanzawa, T., "Oxidation of Ethylene in Shock Tube," *Astronautica Acta*, Vol. 18, 1973, pp. 359–365.

[65]Myers, B. F., and Bartle, E. R., "Reaction and Ignition Delay Times in the Oxidation of Propane," *AIAA Journal*, Vol. 7, No. 10, 1969, pp. 1862–1869.

[66]Petersen, E. L., Davidson, D. F., and Hanson, R. K., "Kinetics Modeling of Shock-Induced Ignition in Low-Dilution CH_4/O_2 Mixtures at High Pressures and Intermediate Temperatures," *Combustion and Flame* (to be published).